PFC/JA-91-1

Elliptically Induced Alfvén Eigenmodes

R. Betti and J. P. Freidberg

January 1991

MIT Plasma Fusion Center
Cambridge, MA 02139

This work was supported by the US DOE Grant No. DE-FG02-91ER-54109.

Submitted for publication in: Physics of Fluids B

Elliptically induced alfvén eigenmodes

R. Betti and J. P. Freidberg

Massachusetts Institute of Technology, Plasma Fusion Center, Cambridge, MA 02139

It is shown that noncircularity of tokamak flux surfaces leads to frequency gaps in the magnetohydrodynamic (MHD) Alfvén continuum. Within these gaps discrete modes having macroscopic structure are shown to exist that have many common features with toroidally induced Alfvén eigenmodes. In particular, both can be driven unstable by a small population of high energy alpha particles. The present work focusses on ellipticity. Since $\kappa - 1 > \epsilon$ in many tokamaks the elliptically induced Alfvén eigenmode may indeed be a more robust mode. The most potentially dangerous mode couples the $m = 1$, $n = 1$ and $m = 3$, $n = 1$ "cylindrical" eigenmodes. The region of strong coupling occurs at the $q(r) = 2$ surface and the width of the coupling region is finite, of order $(\kappa - 1)a$. For typical $q(r)$ profiles, continuum damping is expected to be weak. The elliptically induced Alfvén eigenmode may play an important role in the design of future ignited tokamaks.

I Introduction

During the past several years there has been increasing interest in the problem of energetic particle-Alfvén wave interactions. These interactions can drive instabilities that may play an important role in (1) the observation of fishbone oscillations in existing tokamaks[1] and (2) the possible enhanced loss of alpha particles in future ignited devices such as CIT and ITER.[2] Specifically, in the latter case it has been shown that MHD Alfvén waves whose frequency ω_A is lower than the alpha diamagnetic frequency $\omega_{*\alpha}$ can be driven unstable by resonant particle interactions. Within this class of instabilities, the current view is that toroidally induced Alfvén eigenmodes (TAE)[3-5] may pose the most serious threat. The TAE instabilities have global structure and a real frequency that lies in a narrow gap in the continuum caused by toroidal mode coupling. Hence they are sometimes called "gap modes."

In the present paper we show that noncircularity as well as toroidicity can lead to the existence of gap modes. We focus attention on ellipticity as this may be the most important effect in tokamaks. In particular, since many tokamaks have a finite elongation ($\kappa - 1 \sim 1$) as compared to a small toroidicity ($\epsilon \ll 1$), the elliptically induced Alfvén eigenmode (EAE) derived here, may indeed be a more robust and potentially dangerous mode than the TAE. A summary of the properties of the EAE mode is given below.

1. The most macroscopic and thus potentially dangerous EAE in a tokamak couples the $m = 1, n = 1$ and $m = 3, n = 1$ "cylindrical" eigenmodes.

2. The region of strong coupling (i.e. the gap) occurs at the radius r_0 corresponding to $q(r_0) \equiv 2$. The existence of the gap itself was first pointed out in Ref. [6].

3. The real frequency of the mode is approximately $\omega_0 = v_a(r_0)/R_0 q(r_0)$. The actual eigenfrequency is shifted slightly from ω_0. The shift can in principle be positive or negative.

4. For the sake of analytic simplicity the ellipticity is ordered small: $\kappa - 1 \sim \epsilon^{1/2}$. Since our results show that $\Delta\omega/\omega_0 \sim \kappa - 1$, the implication is that finite ellipticity leads to finite frequency shift. Similarly, the width of the coupling layer scales as $\Delta r/r_0 \sim \kappa - 1$

indicating a region of finite extent.

5. Finally, for typical tokamak profiles satisfying $1 < q(r) < 3$, the eigenfrequency ω_0 does not intersect the continua of $m = 1, m = 3$ or any other ellipticity induced m number, over the entire radius $0 < r < a$. Thus, the continuum damping is recently shown to be important for the TAE[7,8] does not directly affect the $m = 1, 3$ EAE. There is, however, a continuum damping when toroidicity is included, as this couples to the $m = 2$ continuum at the $q = 4/3$ surface. Even so, since the $m = 2$ coupling takes place near the center of the plasma (where electron Landau damping is small), this should not be a big effect.

These results are derived in the main body of the text. The analysis consists of a general formulation of the noncircular gap mode equations, followed by an analytical derivation of the EAE eigenfrequency utilizing an asymptotic matching procedure. Many of the details are similar to those first presented in Ref. [3]. The calculation of the growth rates in the presence of alpha particles is a rather complicated task and the results will be presented in a forthcoming paper.

II Model

The basic equation describing Alfvén gap modes in a noncircular tokamak is derived from the standard MHD Lagrangian $\mathcal{L} \equiv \delta W - \omega^2 K$. In order to carry out the analysis we introduce the ohmic tokamak aspect ratio expansion, $\beta \sim \epsilon^2$, $q \sim 1$, $\beta_p \sim 1$. The derivation requires that $\mathcal{L}$ be calculated to third order in ϵ: $\mathcal{L} = \epsilon^2 \mathcal{L}_2 + \epsilon^3 \mathcal{L}_3 + \ldots$

The analysis begins with the following forms for the potential and kinetic energies,

$$\delta W = \frac{1}{2} \int d\mathbf{r} \Big[|\mathbf{Q}_\perp|^2 + B^2 \, |\nabla \cdot \boldsymbol{\xi}_\perp + 2 \, \boldsymbol{\xi}_\perp \cdot \boldsymbol{\kappa}|^2 + \gamma p \, |\nabla \cdot \boldsymbol{\xi}|^2$$

$$-2(\boldsymbol{\xi}_\perp \cdot \nabla p)(\boldsymbol{\kappa} \cdot \boldsymbol{\xi}_\perp^*) - \frac{J_\parallel}{B}(\boldsymbol{\xi}_\perp^* \times \mathbf{B}) \cdot \mathbf{Q}_\perp \Big] \tag{1}$$

$$K = \frac{1}{2} \int d\mathbf{r} \, \rho \, |\boldsymbol{\xi}|^2. \tag{2}$$

The modes of interest are low n number shear Alfvén waves characterized by $\omega^2 \sim k_\parallel^2 v_a^2$. Since $k_\parallel a \sim \epsilon$, we are required to order $\nabla \cdot \boldsymbol{\xi}_\perp \sim \epsilon\, \boldsymbol{\xi}_\perp / a$, or else the magnetic compression term would dominate the behavior. This implies that $\xi_\parallel \sim \epsilon^2 \xi_\perp$ from which it then follows that the plasma compressibility $\gamma p |\nabla \cdot \boldsymbol{\xi}|^2$, and the parallel kinetic energy $\rho |\xi_\parallel|^2$ both give rise to contributions in $\boldsymbol{\mathcal{L}}$ of order ϵ^4. Thus, both terms can be neglected.

The first step in the derivation is to minimize the magnetic compressibility term order by order. The value of $\nabla \cdot \boldsymbol{\xi}_\perp$ correct to the required accuracy is found by noting that the curvature $\boldsymbol{\kappa} = -\mathbf{e}_R/R + O(\epsilon^2)/a$. This yields

$$\nabla \cdot \boldsymbol{\xi}_\perp \approx \frac{2\xi_R}{R}. \tag{3}$$

Equation (3) can be solved by introducing a stream function as follows

$$\boldsymbol{\xi}_p = R \nabla_p X \times \mathbf{e}_\phi \tag{4}$$

where $\boldsymbol{\xi}_p = (\xi_R, 0, \xi_Z)$ is the poloidal component of $\boldsymbol{\xi}_\perp$ and ∇_p is the poloidal gradient. The toroidal component ξ_ϕ is of order $\xi_\phi \sim \epsilon \xi_p$ and never enters the calculation, even when evaluating $\boldsymbol{\mathcal{L}}$ to order ϵ^3. The entire analysis is now expressed in terms of the single scalar unknown $X = X(R, Z) \exp(-i\omega t - in\phi)$.

The remaining terms in δW and K can be evaluated in a straightforward manner. For the kinetic energy we obtain

$$\rho |\boldsymbol{\xi}_\perp|^2 = \rho R^2 |\nabla_p X|^2. \tag{5}$$

The evaluation of δW requires the quantity $\mathbf{Q}_\perp$, which after a short calculation can be written as

$$\mathbf{Q}_\perp \equiv (\nabla \times \boldsymbol{\xi}_\perp \times \mathbf{B})_\perp = \frac{1}{F_0} \nabla [R^2 \mathbf{B} \cdot \nabla X] \times \mathbf{B} \tag{6}$$

where $F(\psi) \equiv RB_\phi = F_0[1 + O(\epsilon^2)]$; that is $F_0 = R_0 B_0 = \text{const}$. The quantity $J_\parallel$ appearing in the kink term reduces to $J_\parallel = J_\phi[1 + O(\epsilon^2)]$ in the aspect ratio expansion. Similarly $\boldsymbol{\kappa} \approx -\mathbf{e}_R/R$ is only needed to leading order in the curvature term.

Upon combining these results we obtain the following form of $\mathcal{L}$ correct up to and including terms of order ϵ^3

$$\mathcal{L} = \int d\mathbf{r} \left[\frac{|\nabla_p V|^2}{R^2} - J_\phi \nabla_p V \cdot \nabla_p X^* \times \mathbf{e}_\phi + 2R^2 p'(\mathbf{B}_p \cdot \nabla_p X) \frac{\partial X^*}{\partial Z} - \omega^2 \rho R^2 |\nabla_p X|^2 \right]. \tag{7}$$

Here, $V = R^2 \mathbf{B} \cdot \nabla X$, $p' = dp(\psi)/d\psi$, $\mathbf{B}_p = (\nabla\psi \times \mathbf{e}_\phi)/R$, and ψ is the equilibrium flux function satisfying the Grad-Shafranov equation. From Eq. (7) it is straightforward to calculate the variation of $\mathcal{L}$ with respect to X. Setting $\delta\mathcal{L} = 0$ leads to an Euler-Lagrange equation that can be expressed as

$$\begin{aligned} \mathbf{B} \cdot \nabla \left[\Delta^*(R^2 \mathbf{B} \cdot \nabla X) \right] + \frac{1}{R} \nabla_p (R J_\phi) \times \mathbf{e}_\phi \cdot \nabla_p (R^2 \mathbf{B} \cdot \nabla X) \\ - 2R^2 \frac{\partial}{\partial Z} (p' \mathbf{B}_p \cdot \nabla_p X) + \omega^2 \nabla_p \cdot (\rho R^2 \nabla_p X) = 0 \end{aligned} \tag{8}$$

where $\Delta^* V \equiv R^2 \nabla \cdot (\nabla V / R^2)$. Equation (8) is the desired form of the basic stability equation for Alfvén gap modes in a general noncircular geometry, consistent with the ohmic tokamak aspect ratio expansion.

III Derivation of the Simplified Gap Mode Equation

The primary aim of the paper is the investigation of gap modes induced by noncircularity. In many noncircular tokamaks the elongation and triangularity are finite (e.g. $\kappa = 1.8, \delta = 0.4$) and thus represent a stronger source of symmetry breaking than toroidicity. The analyses of these modes, as described by Eq. (8), is significantly simplified by introducing a subsidiary expansion in which the noncircularity is assumed small, although not as small as toroidicity. Specifically, we focus attention on elongation and order κ as follows

$$\kappa - 1 \sim \epsilon^{1/2}. \tag{9}$$

This ordering reduces Eq. (8) to its noncircular, infinite aspect ratio form where all toroidal effects are ignored. (However, the toroidal expansion must be maintained when calculating resonant particle growth rates.) In terms of the original Lagrangian formulation $\mathcal{L} =$

$\epsilon^2\mathcal{L}_2 + \epsilon^3\mathcal{L}_3$, the subsidiary expansion neglects $\mathcal{L}_3$ and assumes $\epsilon^2\mathcal{L}_2$ can be rewritten as $\epsilon^2\mathcal{L}_2 = \epsilon^2(\mathcal{L}_{20} + \epsilon^{1/2}\mathcal{L}_{21}\ldots)$. Equivalently, Eq. (8) neglecting toroidicity but including the full $\mathcal{L}_2$, reduces to

$$\mathbf{B}\cdot\nabla[\nabla_p^2(\mathbf{B}\cdot\nabla X)] + \nabla_p J_\phi \times e_\phi \cdot \nabla_p(\mathbf{B}\cdot\nabla X) + \omega^2\nabla_p\cdot(\rho\nabla_p X) = 0. \tag{10}$$

This equation is similar to that derived in Ref. [9] whose main concern is kink instabilities in elliptical plasmas.

The subsidiary expansion can be conveniently substituted into Eq. (10) by introducing a set of normalized flux coordinates as follows. The equilibrium flux function, satisfying the Grad-Shafranov equation, is written as $\psi = \psi_0(r) + \psi_1(r)\cos 2\theta$ where $\psi_1/\psi_0 \sim \epsilon^{1/2}$ and (r,θ) are the usual toroidal coordinates $R = R_0 + r\cos\theta, Z = r\sin\theta$. The flux coordinates (r',θ') are defined by

$$\begin{aligned} r' &= r - \Delta(r)\cos 2\theta \\ \theta' &= \theta + \frac{\Delta(r)}{r}\sin 2\theta \end{aligned} \tag{11}$$

where $\Delta(r) \equiv -\psi_1/\psi_0' \sim \epsilon^{1/2}a$. The elliptical distortion Δ can be easily shown[10] to satisfy the perturbed Grad-Shafranov equation given by

$$\begin{aligned} &\frac{d}{dr}\left(rB_\theta^2\frac{d\Delta}{dr}\right) - 3\frac{B_\theta^2}{r}\Delta = 0 \\ &\Delta(0) = 0, \quad \Delta(a) = -a(\kappa-1)/2. \end{aligned} \tag{12}$$

Here $B_\theta(r)$ is the zeroth order poloidal magnetic field, which is assumed to be specified as a free function. We shall assume that Eq. (12) has been solved either analytically or numerically and thus $\Delta(r)$ is hereafter treated as a known quantity.

From Eq. (11), it is straightforward to show that

$$\mathbf{B}\cdot\nabla = -iB_0k_\parallel - B_\theta\frac{d}{dr'}\left(\frac{\Delta}{r'}\right)\cos 2\theta'\frac{\partial}{\partial\theta'} \tag{13}$$

where $k_\parallel$ is the operator

$$k_\parallel = \frac{1}{R_0}(n + \frac{i}{q}\frac{\partial}{\partial\theta'}) \tag{14}$$

and $q(r') = r'B_0/R_0B_\theta$ is the safety factor. Similarly, the ∇^2 operator can be written as

$$\nabla^2 = \frac{1}{r'}\frac{\partial}{\partial r'}r'\frac{\partial}{\partial r'} + \frac{1}{r'^2}\frac{\partial^2}{\partial \theta'^2} - 2\frac{d\Delta}{dr'}\cos 2\theta'\frac{\partial^2}{\partial r'^2}. \tag{15}$$

The last terms in Eqs. (13) and (15) represent the $\epsilon^{1/2}$ corrections. Actually, in Eq. (15) there are additional $\epsilon^{1/2}$ terms involving first and zeroth order derivatives with respect to r'. In analogy with previous analysis of gap modes we anticipate that the $\epsilon^{1/2}$ corrections are only going to be important in a narrow region of physical space corresponding to the frequency gap. Thus, it suffices to maintain only the highest derivative $\partial^2/\partial r'^2$ terms in the corrections to ∇^2. In contrast, the operator $\mathbf{B}\cdot\nabla$ has no radial derivative terms because of the introduction of flux coordinates.

The subsidiary expansion and the flux coordinates are now substituted into Eq. (10). After a short calculation we obtain

$$(L_0 + L_1)X = 0 \tag{16}$$

where the operators L_0 and L_1 have the form

$$L_0X \equiv \omega^2\nabla_0\cdot(\rho\nabla_0 X) - B_0^2k_\parallel(\nabla_0^2k_\parallel X) + \frac{iB_0}{r}\frac{dJ}{dr}k_\parallel\frac{\partial X}{\partial\theta} \tag{17}$$

$$L_1X \equiv -2\omega^2\rho\frac{d\Delta}{dr}\cos 2\theta\frac{\partial^2 X}{\partial r^2} + 2B_0^2\frac{d\Delta}{dr}k_\parallel\left(\cos 2\theta\, k_\parallel\frac{\partial^2 X}{\partial r^2}\right)$$
$$+iB_0B_\theta\frac{d}{dr}\left(\frac{\Delta}{r}\right)\left[\cos 2\theta\, k_\parallel\frac{\partial}{\partial\theta}\frac{\partial^2 X}{\partial r^2} + k_\parallel\left(\cos 2\theta\frac{\partial}{\partial\theta}\frac{\partial^2 X}{\partial r^2}\right)\right]. \tag{18}$$

In these expressions the primes have been suppressed from (r', θ') and

$$J = \frac{1}{r}\frac{d}{dr}rB_\theta$$
$$\nabla_0^2 = \frac{1}{r}\frac{\partial}{\partial r}r\frac{\partial}{\partial r} + \frac{1}{r^2}\frac{\partial^2}{\partial\theta^2}. \tag{19}$$

Equation (16) can be solved by Fourier analyzing X in the angle θ:

$$X(r,\theta) = \sum_\ell X_p(r)e^{ip\theta}. \tag{20}$$

Here, $p = m + 2\ell$, m is the fundamental mode number, and the different ℓ harmonics represent the coupling due to noncircularity. Substituting into Eq. (16) yields the following equation for the p'th harmonic

$$D_p X_p + D_{p+2} X_{p+2} + D_{p-2} X_{p-2} = 0 \tag{21}$$

where the D operators have the form

$$\begin{aligned}
D_p &\equiv \frac{1}{r}\frac{d}{dr} r(\omega^2\rho - k_p^2 B_0^2)\frac{d}{dr} - \frac{1}{r^2}\left[p^2(\omega^2\rho - k_p^2 B_0^2) - rB_0^2\frac{dk_p^2}{dr}\right] \\
D_{p+2} &\equiv -\left[(\omega^2\rho - k_p k_{p+2} B_0^2)\frac{d\Delta}{dr} + \frac{1}{2}(p+2)rB_0 B_\theta (k_p + k_{p+2})\frac{d}{dr}\left(\frac{\Delta}{r}\right)\right]\frac{d^2}{dr^2} \\
D_{p-2} &\equiv -\left[(\omega^2\rho - k_p k_{p-2} B_0^2)\frac{d\Delta}{dr} + \frac{1}{2}(p-2)rB_0 B_\theta (k_p + k_{p-2})\frac{d}{dr}\left(\frac{\Delta}{r}\right)\right]\frac{d^2}{dr^2}
\end{aligned} \tag{22}$$

and $k_p = (1/R_0)(n - p/q)$.

Note that D_{p-2}, D_{p+2} are small by order $\epsilon^{1/2}$ compared to D_p. Thus, over most of the cross section the $D_{p\pm 2}$ terms can be neglected. However, if these terms are neglected everywhere, then whenever $\omega^2\rho = k_p^2 B_0^2$ the coefficient of the highest derivative in D_p vanishes and $(D_p)^{-1}$ does not exist; that is, there are no discrete modes, only a continuum.

The regions where coupling is most important can be found by plotting curves of $k_p R_0$ vs q for various ℓ as shown in Fig. 1 (dashed curves) for the case $n = 1, m = 1$. Observe that the $\ell = 0$ and $\ell = 2$ curves intersect at the $q = 2$ surface where $k_1(q = 2) = -k_3(q = 2) = 1/2R_0$. For arbitrary m, n strong coupling occurs when $q_0 = (m+1)/n, k_m = -k_{m+2} = 1/q_0 R_0$, and $\omega_0 = v_a(r_0)/q_0 R_0$.

Consider now a mode with X_m, X_{m+2} as the two dominant harmonics and neglect all others. In the potentially singular region near $q = q_0$, the terms with the highest derivatives for the m and $m+2$ harmonics are given by

$$\begin{aligned}
(\omega^2\rho - k_m^2 B_0^2)\frac{d^2 X_m}{dr^2} - 2\omega^2\rho\frac{d\Delta}{dr}\frac{d^2 X_{m+2}}{dr^2} + \ldots = 0 \\
(\omega^2\rho - k_{m+2}^2 B_0^2)\frac{d^2 X_{m+2}}{dr^2} - 2\omega^2\rho\frac{d\Delta}{dr}\frac{d^2 X_m}{dr^2} + \ldots = 0
\end{aligned} \tag{23}$$

If the determinant of these terms vanishes for any value of r, the equations cannot be inverted and no discrete modes are possible. The frequencies for which the determinant vanishes are given by

$$\omega^2(r) = \frac{v_a^2}{2(1-4\Delta'^2)}\left\{k_m^2 + k_{m+2}^2 \pm \left[(k_m^2 - k_{m+2}^2)^2 + 16\Delta'^2 k_m^2 k_{m+2}^2\right]^{1/2}\right\} \tag{24}$$

$$\approx \frac{v_a^2}{q^2 R_0^2}\left\{1 \pm 2\left[(m+1)^2(1-\frac{q_0}{q})^2 + \Delta'^2\right]^{1/2}\right\}$$

where the second form is obtained by explicitly expanding about the $q = q_0$ surface. Observe that as r varies between $0 < r < a$, there is a narrow band of frequencies centered about $\omega = v_a/qR_0, q = q_0$, for which the determinant *does not* vanish. This is the frequency "gap" shown as the solid curve in Fig. 1. Its boundaries are determined by setting $q = q_0$, corresponding to the throat of the gap.

$$\frac{v_a}{q_0 R_0}(1-\Delta') < \omega < \frac{v_a}{q_0 R_0}(1+\Delta'). \tag{25}$$

Within this range, the determinant does not vanish, and the differential operators in Eq. (23) can be inverted. Thus, if a discrete mode does exist, its frequency must satisfy Eq. (25). To determine the actual existence of such a mode, it is necessary to solve the full equations over the entire plasma $0 < r < a$. In this connection, note from Fig. 1 that for typical tokamaks satisfying $1 < q(r) < 3$, the frequency ω_0 does not intersect the $m = 1, m = 3$ or any $m = 1 + 2\ell$ continuum at any value of $r \leq a$. Thus continuum damping which has been shown to be important for the TAE is not expected to be so for the EAE.

A simplified form of the full equations is obtained by assuming the mode consists primarily of the X_m and X_{m+2} harmonics, and evaluating the small operators $D_{p\pm 2}$ at r_0 corresponding to the $q = q_0$ surface. For simplicity the density $\rho(r)$ is assumed constant: $\rho = \rho_0$. It is also convenient to introduce new variables ξ_m and ξ_{m+2} defined by $X_m = r\xi_m, X_{m+2} = r\xi_{m+2}$. Equation (21) for the $(m, m+2)$ harmonics reduces to

$$D_m \xi_m + F\xi_{m+2} = 0 \tag{26a}$$

$$D_{m+2}\xi_{m+2} + F\xi_m = 0. \tag{26b}$$

The operator D_p is given by

$$D_p \equiv \frac{1}{r}\frac{d}{dr}r^3(\omega^2\rho_0 - k_p^2 B_0^2)\frac{d}{dr} - (p^2-1)(\omega^2\rho_0 - k_p^2 B_0^2). \tag{27}$$

The operator F is slightly subtle. Straightforward substitution yields

$$F\xi_p = -2\omega^2\rho_0\Delta'(r_0)(r^2\xi_p')'. \tag{28}$$

However, under our previous assumption that the correction terms are only important in a narrow layer where the highest derivatives dominate, we maintain consistency by writing

$$F\xi_p \approx -2\omega_0^2\rho_0\Delta'(r_0)r_0^2\xi_p''. \tag{29}$$

The errors made by this approximation are of the same order as those already neglected in the derivation of the $D_{p\pm2}$ operators.

Equations (26)-(29) describe gap modes in weak noncircular geometries.

IV Asymptotic Matching Solutions

The gap mode equations can be solved by a standard asymptotic matching procedure. The analysis is similar but more general than that originally given by the Princeton group.[3]

A The Layer Region

The first step is to simplify Eq. (26) in the layer region. We introduce normalized quantities

$$x = \frac{r - r_0}{r_0}$$
$$\omega^2 = \omega_0^2(1 + 2\Omega) \tag{30}$$

where r_0 is the layer radius and Ω is the new eigenvalue. Under our previous ordering assumptions $\Omega \ll 1$ and $x \ll 1$. It then follows that in the vicinity of the layer

$$\begin{aligned} \frac{1}{q} &\approx \frac{1}{q_0}(1 - sx) \\ k_m^2 &\approx \frac{1}{R_0^2 q_0^2}(1 + 2msx) \\ k_{m+2}^2 &\approx \frac{1}{R_0^2 q_0^2}\left[1 - 2(m+2)sx\right]. \end{aligned} \tag{31}$$

Here, $s = r_0 q'(r_0)/q(r_0)$ is the shear at the layer. Equation (26) reduces to

$$\begin{aligned} \frac{d}{dx}(\Omega - msx)\frac{d\xi_m}{dx} - \Delta_0' \frac{d^2\xi_p}{dx^2} &= 0 \\ \frac{d}{dx}(\Omega + psx)\frac{d\xi_p}{dx} - \Delta_0' \frac{d^2\xi_m}{dx^2} &= 0. \end{aligned} \tag{32}$$

In these equations $p = m + 2$ and $\Delta_0' \equiv d\Delta(r_0)/dr_0$ is dimensionless.

Equation (32) can be easily solved, yielding

$$\begin{aligned} \xi_m &= \frac{1}{m^{1/2}}\left[\frac{C_p + \lambda C_m}{(1-\lambda^2)^{1/2}}\alpha - C_m \ln\cos\alpha + A_m\right] \\ \xi_p &= \frac{1}{p^{1/2}}\left[\frac{C_m + \lambda C_p}{(1-\lambda^2)^{1/2}}\alpha + C_p \ln\cos\alpha + A_p\right] \end{aligned} \tag{33}$$

where A_m, A_p, C_m, C_p are four free integration constants,

$$\lambda = \frac{m+1}{(mp)^{1/2}}\frac{\Omega}{\Delta_0'} \tag{34}$$

is a new form of the normalized eigenvalue Ω, and

$$x = \frac{\Delta_0'}{s(mp)^{1/2}}\left[\frac{\lambda}{m+1} + (1-\lambda^2)^{1/2}\tan\alpha\right] \tag{35}$$

defines the new independent variable α. Equation (33) represents the desired solution in the layer region.

The second step in the analysis is to solve for the solutions in the exterior regions, which satisfy

$$\begin{aligned} \frac{1}{r}\frac{d}{dr}r^3 f_m \frac{d\hat{\xi}_m}{dr} - (m^2-1)f_m\hat{\xi}_m = 0 \\ \\ \frac{1}{r}\frac{d}{dr}r^3 f_p \frac{d\hat{\xi}_p}{dr} - (p^2-1)f_p\hat{\xi}_p = 0 \end{aligned} \tag{36}$$

where $f_m = \omega_0^2\rho_0 - k_m^2 B_0^2$, $f_p = \omega_0^2\rho_0 - k_p^2 B_0^2$ and the $\hat{}$ denotes exterior region. Near the layer, these equations reduce to

$$\begin{aligned} \frac{d}{dx}x\frac{d\hat{\xi}_m}{dx} = 0 \\ \\ \frac{d}{dx}x\frac{d\hat{\xi}_p}{dx} = 0. \end{aligned} \tag{37}$$

The solutions to Eq. (37) are given by

$$\begin{aligned} \hat{\xi}_m^+ = K_m^+\left[\frac{1}{2}\ln x^2 + b_m^+\right] \qquad \hat{\xi}_m^- = K_m^-\left[\frac{1}{2}\ln x^2 + b_m^-\right] \\ \\ \hat{\xi}_p^+ = K_p^+\left[\frac{1}{2}\ln x^2 + b_p^+\right] \qquad \hat{\xi}_p^- = K_p^-\left[\frac{1}{2}\ln x^2 + b_p^-\right]. \end{aligned} \tag{38}$$

The superscripts $(+)$ and $(-)$ refer to the regions between the layer and $r = a$, and the layer and the origin respectively. The constants K_m and K_p are free integration constants. The coefficients b_m and b_p represent the fraction of "constant solution" to "logarithmic solution" near the layer. These coefficients are in principle known. For instance b_m^- can be obtained by integrating the exact exterior equation [Eq. (36)] from the origin towards the singular layer $r = r_0$, using the regularity boundary condition at $r = 0$. The coefficient b_m^- is found numerically by computing

$$b_m^- = \underset{r\to r_0^-}{L}\left[\frac{\hat{\xi}_m^-}{x\hat{\xi}_m^{-\prime}} - \frac{1}{2}\ln x^2\right]. \tag{39}$$

A similar calculation yields b_m^+. The only difference is that in this case Eq. (36) must be integrated inward from the boundary $r = a$, using $\hat{\xi}_m^+(a) = 0$. In this case

$$b_m^+ = \underset{r \to r_0^+}{L} \left[\frac{\hat{\xi}_m^+}{x\hat{\xi}_m^{+\prime}} - \frac{1}{2} \ln x^2 \right]. \tag{40}$$

Equations (39) and (40) also yield b_p^- and b_p^+ by replacing m by p.

Another approach to calculate b_m and b_p is by variational techniques, as demonstrated in Appendix A. The result is a set of explicit integral expressions for these coefficients that can be easily evaluated for any given q profile.

Based on the above discussion we shall hereafter assume that $b_m^-, b_p^-, b_m^+, b_p^+$ are known quantities, and that the desired exterior solutions in the vicinity of the layer are given by Eq. (38).

V The Dispersion Relation

The eigenfrequency of the gap mode is obtained by asymptotically matching the solutions across the layer as follows,

$$\begin{aligned} \hat{\xi}_m^-(x \to 0) = \xi_m(x \to -\infty) \qquad \xi_m(x \to \infty) = \hat{\xi}_m^+(x \to 0) \\ \hat{\xi}_p^-(x \to 0) = \xi_p(x \to -\infty) \qquad \xi_p(x \to \infty) = \hat{\xi}_p^+(x \to 0). \end{aligned} \tag{41}$$

It is straightforward to show that in the limit $x \to \pm\infty$ the layer solutions given by Eq. (33) have the same functional form (i.e. $c_1 + c_2 \ln x^2$) as the exterior solutions. This is a direct consequence of Eq. (35): that is, as $x \to \pm\infty$ then $\alpha \to \pm\pi/2$ and $\cos\alpha \to \pm\eta/x$ where $\eta = \Delta_0'(1-\lambda^2)^{1/2}/s(mp)^{1/2}$.

The first step in the matching is to equate the coefficients of the logarithmic terms. This yields

$$\begin{aligned} K_m^+ = K_m^- = \frac{C_m}{m^{1/2}} \\ K_p^+ = K_p^- = \frac{C_p}{p^{1/2}}. \end{aligned} \tag{42}$$

The second step in the matching is to equate the coefficients of the constant terms. After eliminating A_m and A_p from this set of relations we are left with two coupled equations for the coefficients C_m and C_p given by

$$\pi \frac{C_p + \lambda C_m}{(1-\lambda^2)^{1/2}} = C_m \Delta b_m$$
$$\pi \frac{C_m + \lambda C_p}{(1-\lambda^2)^{1/2}} = -C_p \Delta b_p \tag{43}$$

where $\Delta b_m = b_m^+ - b_m^-$, $\Delta b_p = b_p^+ - b_p^-$.

The dispersion relation for λ is obtained by setting the determinant to zero. A short calculation yields

$$\frac{\omega}{\omega_0} = 1 + \frac{m^{1/2}(m+2)^{1/2}}{m+1} \frac{\delta}{(1+\delta^2)^{1/2}} \Delta_0' \tag{44}$$

with

$$\delta = \frac{\pi^2 + \Delta b_{m+2} \Delta b_m}{\pi(\Delta b_{m+2} - \Delta b_m)}. \tag{45}$$

Note that δ can in general have either sign indicating that the frequency may be shifted in either direction with respect to ω_0. Also, note that for the special case of $m = 1$, Eq. (36) can be solved exactly, leading to the result that $b_m^- = \infty$. Thus, for $m = 1$, Eq. (45) simplifies to

$$\delta = -\frac{\Delta b_{m+2}}{\pi}. \tag{46}$$

The calculation of the asymptotically matched eigenfunctions and the corresponding eigenvalue Ω proves that an ellipticity induced gap mode does indeed exist.

VI Conclusions

We have demonstrated the existence of elliptically induced Alfvén eigenmodes. These modes are of the same general class as the toroidally induced Alfvén eigenmode. In configurations with finite ellipticity, the EAE has a global structure centered about the $q = (m+1)/n$ surface. The region of "localization" is of order $\kappa - 1$ which is often much larger than ϵ. Thus, the EAE may be more robust than the TAE in such configurations.

The EAE as well as the TAE can be excited by resonance with circulating alpha particles[3,5]. The details of the mode excitation have been investigated and will be presented elsewhere. These studies indicate that growth or damping depends upon a competition between the alpha particle driver, electron Landau damping and continuum damping[7,8] (as first pointed out for the TAE mode). Continuum damping is weaker for the EAE mode as there is no interaction with the continuum for typical q profiles satisfying $q(a) \sim 3$, even when density profile effects are taken into account. See Fig. 1. Our stability studies also show that perhaps unexpectedly, ion Landau damping may have a substantial stabilizing effect on the TAE. The effect on the EAE is much weaker. Both the TAE and EAE need further investigation to determine how detrimental their effect may be on alpha particle confinement in ignited tokamaks.

Appendix A

The coefficient b_m can be accurately estimated by variational techniques. The appropriate Lagrangians for b_m^- and b_m^+, corresponding to Eq. (36), are given by

$$\mathcal{L}^- = \int_0^{1-\epsilon} y f_m \left[y^2 \xi_m'^2 + (m^2-1)\xi_m^2 \right] dy - c^2 f_m'(1) \ln \epsilon \tag{A1}$$

$$\mathcal{L}^+ = \int_{1+\epsilon}^{k} y f_m \left[y^2 \xi_m'^2 + (m^2-1)\xi_m^2 \right] dy + c^2 f_m'(1) \ln \epsilon \tag{A2}$$

where $y = r/r_0, k = a/r_0$ and in Eqs. (A1) and (A2), $c = 1/b_m^-$ and $c = 1/b_m^+$ respectively. This variational principle is valid only if ξ_m satisfies the following two conditions. First, near the singular layer

$$\xi_m(y) = 1 + c \ln |y-1|. \tag{A3}$$

Second, ξ_m must be properly normalized by choosing the solutions at $r = 0$ and $r = a$ to be regular, with amplitude independent of c: that is, $\xi_m(0) \approx a_1 y^{m-1}$ and $\xi_m(k) \approx a_2(k-y)$ with a_1 and a_2 independent of c.

In the analysis c is treated as a variational parameter to be evaluated in the limit $\epsilon \to 0$. The validity of the variational principle can be easily verified by standard techniques using the relations $\delta\xi(1) = \delta c \ln \epsilon$ [from Eq. (A3)] and $\delta\xi(k) = 0$ (from the normalization). A convenient choice of trial functions is as follows

$$\begin{aligned} \xi_m^- &= \xi_1(y) + c\xi_2(y) \\ \xi_m^+ &= \xi_3(y) + c\xi_4(y) \end{aligned} \tag{A4}$$

where

$$\begin{aligned} \xi_1 &= y^{m-1} \\ \xi_2 &= y^{m+1} \ln\left(\frac{1-y^2}{2}\right) \\ \xi_3 &= y^{-m-1}\left(\frac{k^{2m}-y^{2m}}{k^{2m}-1}\right) \\ \xi_4 &= y^{-m-1}\left(\frac{k^{2m}-y^{2m}}{k^{2m}-1}\right)\left(\frac{k^2-y^2}{k^2-1}\right) \ln\left(\frac{y^2-1}{2}\right). \end{aligned} \tag{A5}$$

Substituting into the Lagrangian yields expressions of the form

$$\mathcal{L} = I_0 + 2cI_1 + c^2 I_2. \tag{A6}$$

Minimizing with respect to c we obtain

$$\begin{aligned} b_m^- &= -I_2^- / I_1^- \\ b_m^+ &= -I_2^+ / I_1^+ \end{aligned} \tag{A7}$$

In the limit $\epsilon \to 0$, the integrals can be written as

$$\begin{aligned} I_1^- &= \int_0^1 y f_m \left[y^2 \xi_1' \xi_2' + (m^2 - 1)\xi_1 \xi_2 \right] dy \\ I_2^- &= \int_0^1 \left\{ y f_m \left[y^2 \xi_2'^2 + (m^2 - 1)\xi_2^2 \right] + \frac{f'(1)}{1-y} \right\} dy \\ I_1^+ &= \int_1^k y f_m \left[y^2 \xi_3' \xi_4' + (m^2 - 1)\xi_3 \xi_4 \right] dy \\ I_2^+ &= \int_1^k \left\{ y f_m \left[y^2 \xi_4'^2 + (m^2 - 1)\xi_4^2 \right] - \frac{f'(1)}{y-1} \right\} dy + f'(1) \ln(k-1). \end{aligned} \tag{A8}$$

Note that in the expression for I_2^- and I_2^+, the integrands are finite as $y \to 1$. Equations (A7) and (A8) are the desired expressions for b_m^- and b_m^+.

References

[1]J. D. Strachan, B. Grek, W. Heidbrink, D. Johnson, S. M. Kaye, H. W. Kugel, B. LeBlanc, K. McGuire, Nucl. Fusion **25**, 863 (1985).

[2]D. J. Sigmar, C. T. Hsu, R. White, C. Z. Cheng, IAEA Technical Committee Meeting on "Alpha Particles/Confinement and Heating," October 1989, Kiev, USSR.

[3]C. Z. Cheng, M. S. Chance, Phys. Fluids **29**, 3659 (1986).

[4]G. Y. Fu, J. W. Van Dam, Phys. Fluids B1, 1949 (1989).

[5]J. W. Van Dam, G. Y. Fu, C. Z. Cheng, Fus. Tech. **18**, 461 (1990).

[6]R. L. Dewar, R. C. Grimm, J. L. Johnson, E. A. Frieman, J. M. Greene, and P. H. Rutherford, Phys. Fluids **17**, 930 (1974).

[7]Z. Guo, H. L. Berk, J. W. Van Dam, D. E. Baldwin, C. Z. Cheng, Bull. Am. Phys. Soc. **35**, 1923 (1990).

[8]F. Zonca, L. Chen, Bull. Am. Phys. Soc. **35**, 2069 (1990).

[9]D. Edery, G. Laval, R. Pellat, J. L. Soulé, Phys. Fluids **19**, 260 (1976).

[10]S. P. Hakkarainen, R. Betti, J. P. Freidberg, R. Gormley, Phys. Fluids **B2**, 1565 (1990).

Figure Captions

Fig. 1 Plot of $\omega(r)R_0/v_a \equiv k_p R_0$ vs $q(r)$ for the following modes (a) $m = 1$, $n = 1$ and $m = 3$, $n = 1$; (b) $m = 2$, $n = 2$ and $m = 4$, $n = 2$; (c) $m = 3$, $n = 3$ and $m = 5$, $n = 3$; (d) $m = 4$, $n = 4$ and $m = 6$, $n = 4$. The dashed lines are the equivalent cylindrical modes while the solid curves represent the fully coupled system.

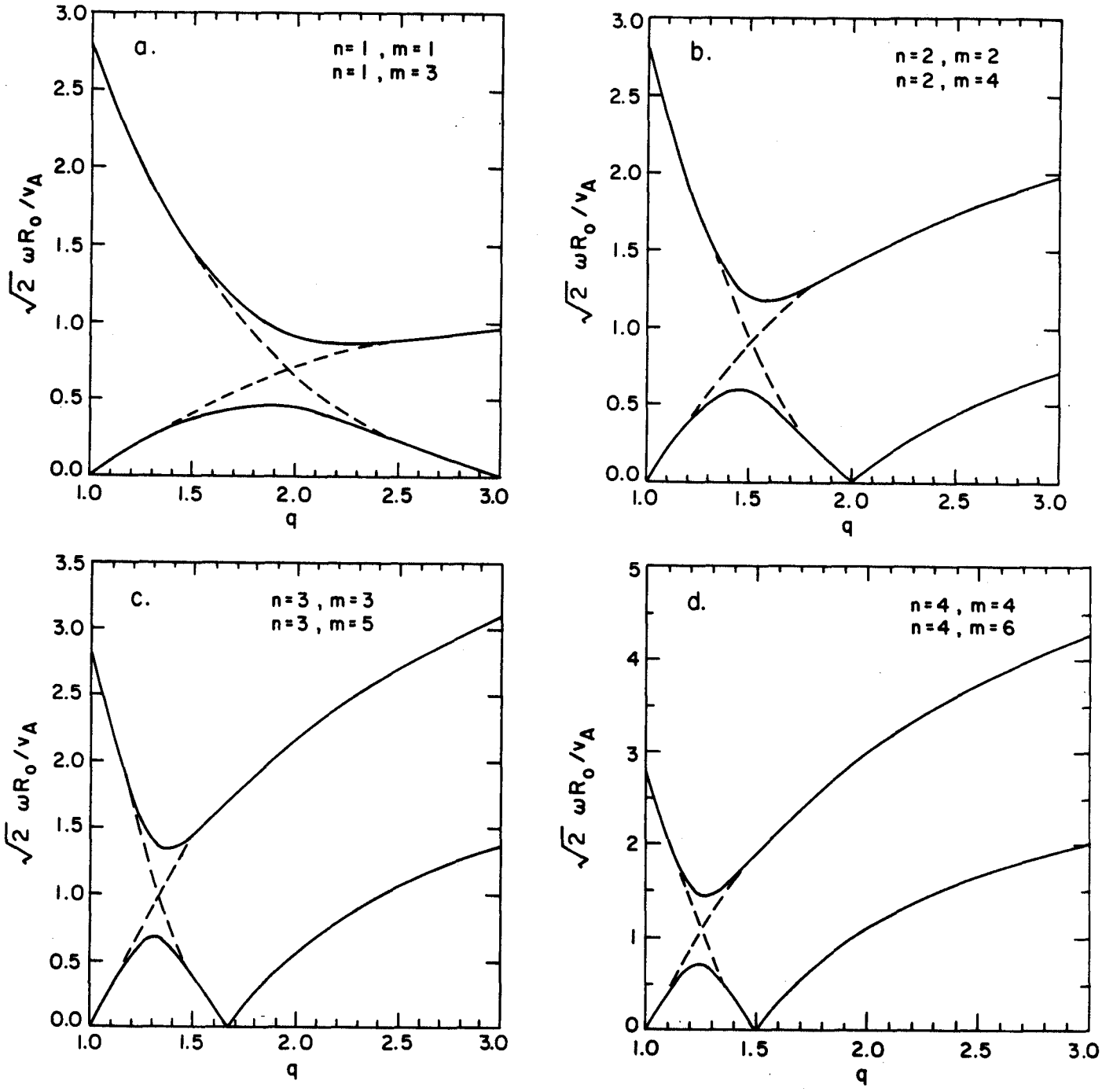
a.
n=1, m=1
n=1, m=3
b.
n=2, m=2
n=2, m=4
c.
n=3, m=3
n=3, m=5
d.
n=4, m=4
n=4, m=6
$\sqrt{2}\ \omega R_0/v_A$
q

Figure 1